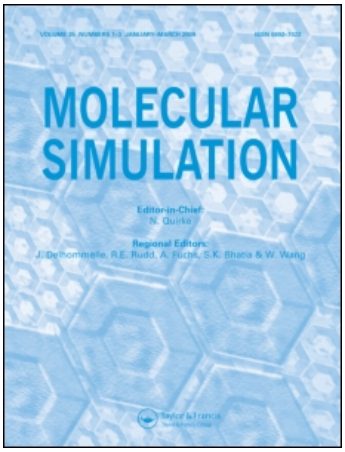

Molecular Simulation
Publication details, including instructions for authors and subscription information:
http://www.informaworld.com/smpp/title~content=t713644482

An insight into the mechanism of the cellulose dyeing process, part 1: Modelling azo-systems in azo-linked aromatics and dyes

Kevin R. Flower[a]; John D. Hamlin[a]; Andrew Whiting[b]
[a] Department of Chemistry, U.M.I.S.T., Manchester, UK [b] Department of Chemistry, Science Laboratories, University of Durham, Durham, UK

Online publication date: 26 October 2010

To cite this Article Flower, Kevin R. , Hamlin, John D. and Whiting, Andrew(2002) 'An insight into the mechanism of the cellulose dyeing process, part 1: Modelling azo-systems in azo-linked aromatics and dyes', Molecular Simulation, 28: 12, 1031 — 1047
To link to this Article: DOI: 10.1080/0892702021000011061
URL: http://dx.doi.org/10.1080/0892702021000011061

Molecular Simulation, 2002 Vol. 28 (12), pp. 1031–1047

AN INSIGHT INTO THE MECHANISM OF THE CELLULOSE DYEING PROCESS, PART 1: MODELLING AZO-SYSTEMS IN AZO-LINKED AROMATICS AND DYES

KEVIN R. FLOWER[a], JOHN D. HAMLIN[a] and ANDREW WHITING[b,*]

[a]*Department of Chemistry, Faraday building, U.M.I.S.T., P.O. Box 88, Manchester, M60 1QD, UK;* [b]*Department of Chemistry, University of Durham, Science Laboratories, South Road, Durham, DH1 3LE, UK*

(Received October 2001; In final form October 2001)

Molecular modelling has been used to model the three-dimensional structure of azo-containing aryl systems and in particular, azo-dyes such as Procion Red MX-5B. These simulations look in detail at the dynamics of the azo-linkage and the effect of an *ortho*-phenol function. In this paper we show that the planar arrangement of the C–N=N–C potentially delocalised sp^2-hybridised system is not encountered exactly in the systems examined; a *transoid*-arrangement of the azo-linkage allows dihedrals to approach close to 180°, however, a *cisoid*-arrangement can engender greater deformation producing dihedrals around 30° away from planarity. Hence, intra-molecular repulsions are capable of easily distorting the azo-linkages producing a range of dihedral geometries which depend strongly on other substituents around the molecular framework.

Keywords: Cellulose; Dyeing; Azo-systems; Tautomer

INTRODUCTION

Azo-compounds have been known for many years and are particularly important in the dyes stuffs industry. Azo-compounds exist in two distinct stereochemical isomeric forms with respect to the azo-function. For example, azo-benzene exists as an equilibrium mixture of the lower energy *E*, or *trans*-isomer and the higher energy, *Z*- or *cis*-form [1,2]. The interconversion between *trans*-form **1** and

*Corresponding author. E-mail: andy.whiting@durham.ac.uk.

ISSN 0892-7022 print © 2002 Taylor & Francis Ltd
DOI: 10.1080/0892702021000011061

cis-form **2** can be induced by exposure to light (Eq. (1)). The degree of conversion is known to be dependent upon the wavelength of light [3]. The degree of conversion of **1**–**2** under these conditions can be appreciable, with 24% of the less stable isomer **2** forming in a few hours from an acetic acid solution of azobenzene upon exposure to sunlight. Reversion to the *trans*-form **1** occurs with heating and can be catalysed by a variety of substances that can function as electron donors or acceptors [4].

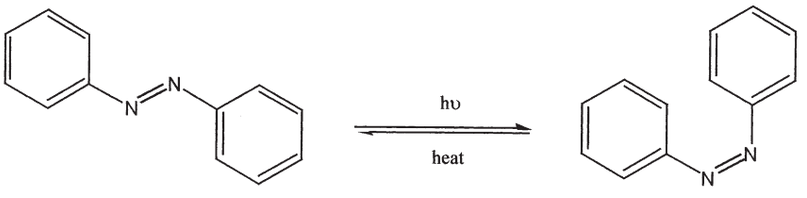

1 **2** (1)

In addition to simple azo-linked compounds typified by **1** and **2**, azo-compounds and dyes can be derived from diazonium salts and phenolic or keto–enol coupling components and are normally depicted in the azo-phenol form, typified by **3**. However, an alternative tautomeric structure **4** can also occur where the azo- and hydroxy-functions are located on adjacent carbon atoms (Eq. (2)). The existence of the alternative tautomer **4**, is known as the hydro-azo form. The actual structure of any particular azo-compound is dependent on the relative energies of the tautomers that are accessible [5].

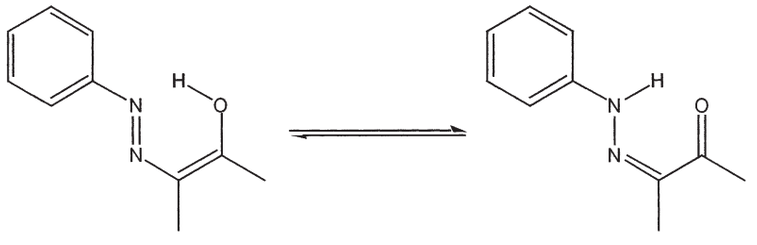

3 **4** (2)

As part of the program aimed at developing an understanding of the role of dye-bath additives in determining dyeing efficiency, we wished to understand the way in which dye molecules interact with each other, with cellulose surfaces and with dye-bath additives [6]. In this paper, we report the first part of this study in which we systematically examine the effects of adding substituents to basic azo-containing compounds versus azo-geometry and tautomerisation.

METHODS

Procion Red MX-5B **5** was chosen as an example dye for this study since it is representative of a whole class of reactive halo-triazinyl reactive dyes. It was suitable for the modelling studies due to the low number of atoms in the molecule and its dying profile being well known. Thus, in principle it should be possible to use molecular modelling to simulate the dyes behaviour throughout the dyeing process, of which there are two main stages: (1) interaction of the dye molecules in solution, and (2) delivery onto the cellulose surface. However, before these two stages could be simulated the fundamental dynamics of azo-linkages needed to be fully understood. Therefore the behaviour of the azo-linkage in **5** and other representative molecules was studied.

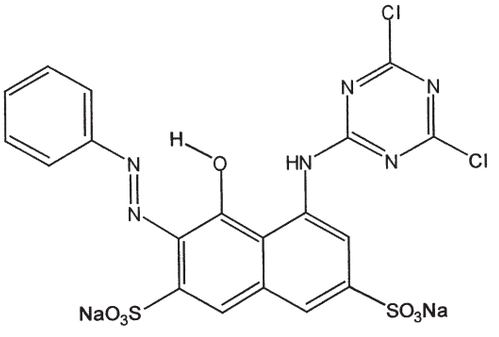

5

The aim of the study was to determine whether the azo-linkage is as rigidly defined as conventional wisdom might dictate, using a combination of minimisation and dynamic simulations on simple azo-functionalised molecules and comparing results obtained to referenced crystallographic data for the same compounds. The comparability of the data would then offer validity for using the CHARMm force field (within QUANTA 97®), used in the molecular modelling, for more extensive simulations and more complex structures.

RESULTS AND DISCUSSION

Most of the crystallographic data that has been published on azo-containing compounds is available from the QUEST crystallographic database [7], and it appears that most crystalline azo-containing compounds do not crystallise as the exclusively *cis* (Ar–N=N–Ar dihedral of 0°) or *trans* (dihedral of 180°) isomer.

It is generally found that in the crystalline state, the Ar–N=N–Ar dihedral angle does approximate to one or other of the extreme conformations. This, however, is not the case for the three compounds **6**–**8** which all have R_1–N=N–R_2 torsion angles that are neither indicative of a *cis* or *trans* conformation. These results are summarised in Table I.

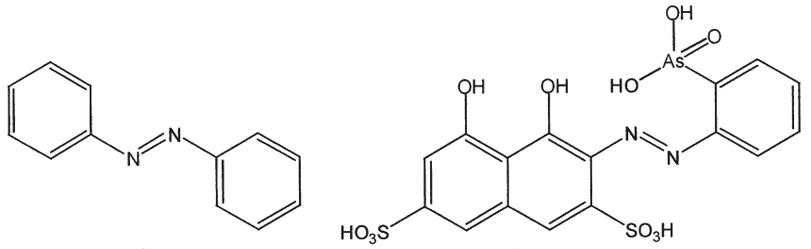

6

7

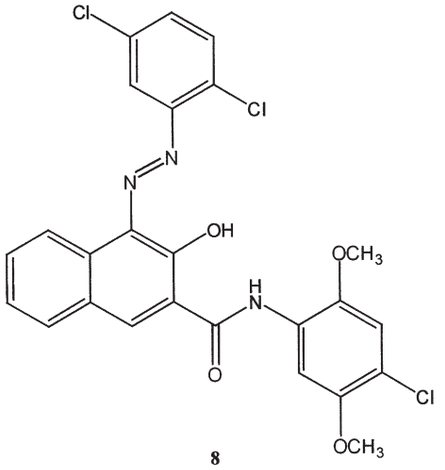

8

In addition, a synthetic study by Flower *et al.* [11] has led to the isolation and elucidation of the crystal structure of 1-(4-methylphenylazo)naphthalene-2-acetate **9**, which is locked to the enol-like form which is in contrast to the

TABLE I Showing the dihedral and associated bond lengths for **6**, **7**, and **8**

		6 [8]	**7** [9]	**8** [10]
Dihedral angle	R_1–*N*=*N*–R_2	332.8	185.0	179.3
Bond length (Å)	–*N*=*N*–	1.696	1.320	1.341
Bond length (Å)	*R*$_1$–*N*=N–R_2	1.494	1.334	1.315
Bond length (Å)	R_1–N=*N*–*R*$_2$	1.494	1.400	1.380

previously published azo-containing compound 1-(4′-*N*,*N*-dimethylaminophenylazo)-2-naphthol **10** which is shown to display the same enol conformation, but can still undergo keto–enol tautomerism [12].

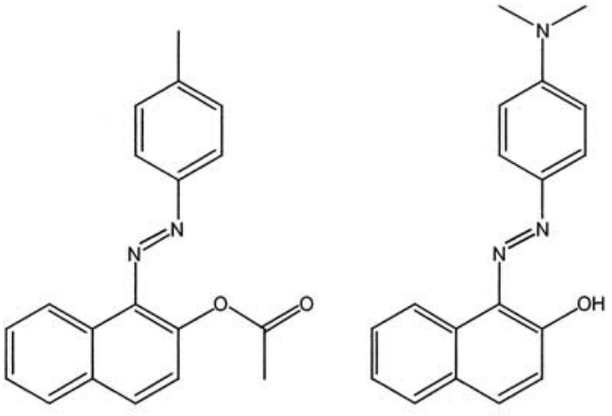

9 **10**

Molecular modelling studies were therefore conducted on the compounds **9** and **10** using the CHARMm force field [13], with the steepest descent (SD) and conjugate gradient (CG) minimisation methods being employed, to determine the structural characteristics of the compounds [14,15]. The minimised structures were then subjected to molecular dynamics simulation procedures [16]. The resulting structures **9*** and **10*** from these experiments are shown in Figs. 1 and 2,

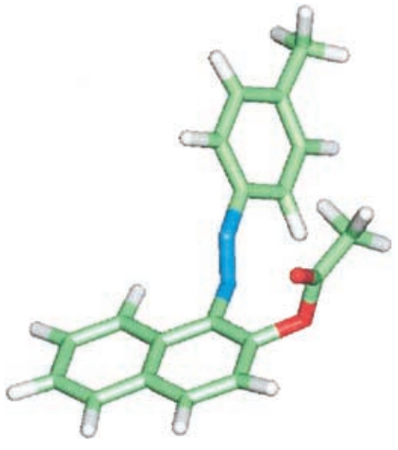

FIGURE 1 Showing compound **9*** after molecular dynamics simulations.

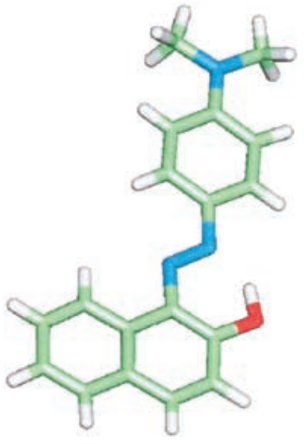

FIGURE 2 Showing compound **10*** after molecular dynamics simulations.

respectively. These calculated structures correspond very closely to the original crystal structures reported by Flower *et al.* [11,12], i.e. bond lengths and angles have a maximum of 4% deviation, when compared with the crystal structures (Table II). These data show that the CHARMm force field, within QUANTA 97®, provides results that correspond well with crystallographically determined azo-containing compounds.

A further study was therefore undertaken to ascertain the conformational variations that are accessible to azo-compounds. Thus, conformational searches were also performed from within QUANTA 97® using each of the structures **11**–**17** (this series of structures was chosen in order to probe the incremental effect of adding substituents to a basic azo-system, through an intact reactive dye system), and Procion Red MX-5B **5**, to gain an insight into the structural characteristics of each of the component parts of the dye molecule. The two dihedral angles of most interest were Φ_1 and Φ_2 (Fig. 3). The conformational analysis was performed using a GRID-scan procedure, in which each of the dihedral angles Φ_1, Φ_2 were

TABLE II Comparing crystallographic and modelled structures reported by Flower *et al.*

		9	**10**	**9***	**10***
Dihedral angle (Φ_1)		180.8	180.7	174.5	181.6
Bond length (Å)	–N=N–	1.240	1.276	1.236	1.238
Bond length (Å)	Aro–N=N–	1.424	1.398	1.381	1.356
Bond length (Å)	Nap–N=N–	1.413	1.399	1.373	1.363

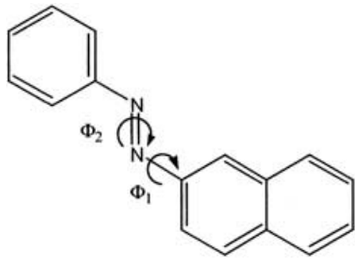

FIGURE 3 Showing the bonds of interest for GRID-scan analysis.

moved through 10° increments until one complete revolution was achieved, this generated 1296 possible conformations for each of the compounds **5** and **11**–**17**.

The result of the GRID-scan conformational analysis were plotted graphically as contour plots Figs. 4–11, with the plot representing a contour of a potential energy surface. The contour lines join points of equal energy and the cross-hair depicts the lowest energy conformation for that structure. From each of these plots it is possible to see the predicted dihedral angles for Φ_1 and Φ_2 for each of the structures **11**–**17**.

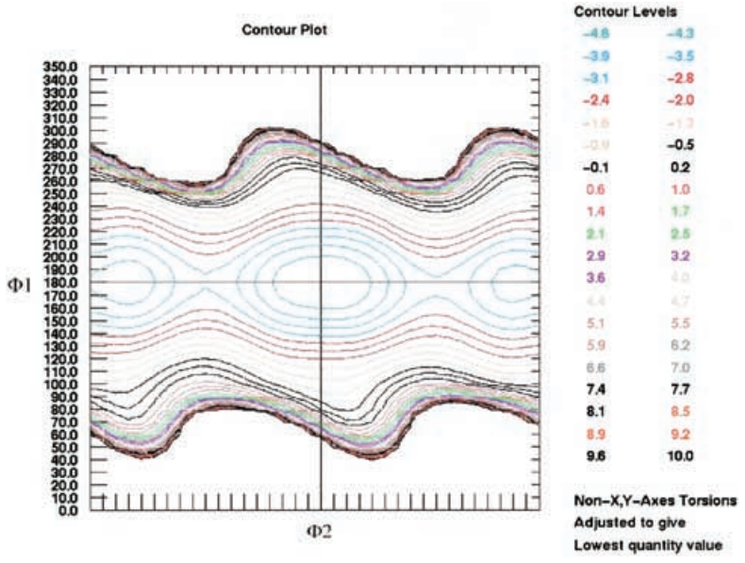

FIGURE 4 Grid-scan plot for phenylazonaphthalene **11**.

In the case of the phenylazonaphthalene **11** the predicted lowest energy conformation has dihedral angles for Φ_1 and Φ_2 of 180 and 180°, respectively

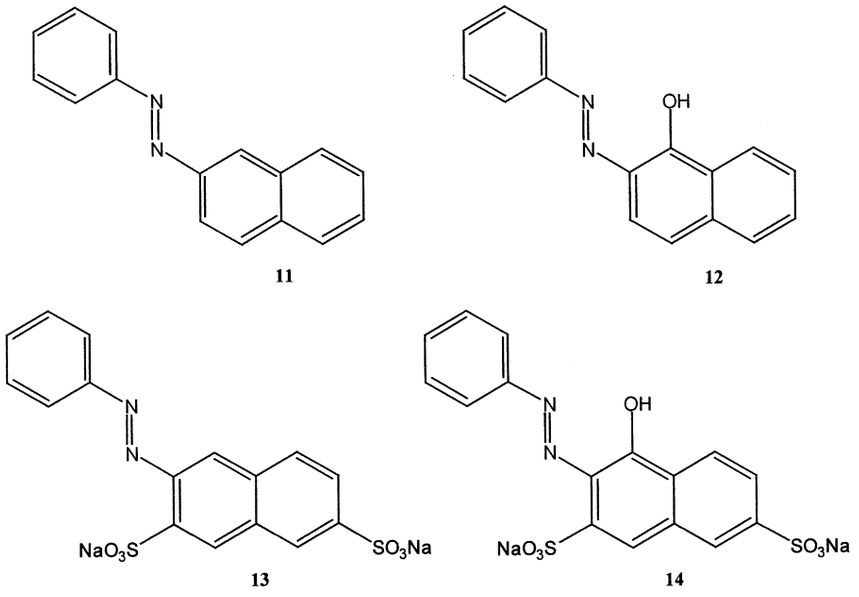

11 **12**

13 **14**

(Fig. 4). The minimised structure **11** determined by dynamics simulation also has a conformation with dihedral angles that approximate to those observed for the GRID-scan conformational search (Table III). The GRID-scan minimum energy conformation having a predicted energy of $-4.63\,\text{kcal mol}^{-1}$ for the whole molecule, as does the molecular dynamics simulation model structure.

The phenylazonaphthalene **11** is fairly sterically unencumbered and the introduction of a hydroxyl group adjacent to the azo-linkage gives phenylazonaphth-1-ol **12**, which causes a marked change in Φ_2 (Fig. 5) (i.e. the Ar–N=N–Ar dihedral). This could be due to a combination of factors one of which is the ability of the hydroxyl to hydrogen bond to one of the azo-nitrogens resulting in keto–enol tautomerisation (Eq. (2)), with the hydrogen bond restricting the conformational flexibility of the resulting molecule.

Two further factors are the steric effect of the hydroxyl function and dipolar repulsion between the oxygen and nitrogen atoms. The addition of two sulphonate groups to the phenylazonaphthalene core **11** to give phenylazonaphthalene-3,6-disulphonate **12**, causes only a small change in the GRID-scan torsion angles (Fig. 6) when compared to the original phenylazonaphthalene **11**. The addition of sulphonates to phenylazonaphth-1-ol **12**, to give phenylazonapth-1-ol-3,6-disulphonate **14**, has little effect on the azo-torsion angles when

compared to those for the hydroxy phenylazonaphthalene **12** core (Fig. 7). Hence, the added complexity of the sulphonate groups play little part in determining the final minimised structure of the Procion Red MX-5B **5**.

The addition of a dihalo-triazinyl ring to the phenylazonaphthalene **11** substructure, to give phenyl-3-azonaphthalene-8-aminodichlorotriazine **15**, had a profound influence upon the GRID-scan plots (Fig. 8), and the dynamics

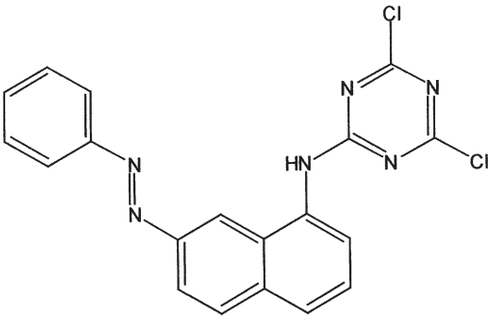

15

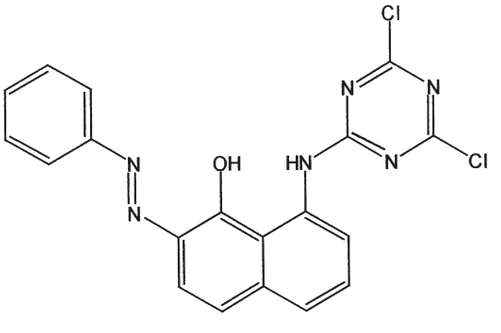

16

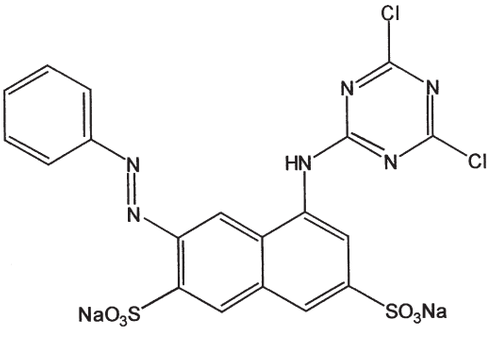

17

TABLE III Comparison of conformation and relative energies by GRID-scan and MD analysis

Structure	*GRID-scan*		*Energy*, *E* (kcal mol^{-1})	*MD*		*Energy*, *E* (kcal mol^{-1})
	Φ_1	Φ_2		Φ_1	Φ_2	
11	180.0	180.0	−4.63	181.1	189.0	−4.63
12	180.0	20.0	1.04	182.7	17.0	1.03
13	200.0	150.0	65.2	202.9	145.5	65.18
14	150.0	240.0	56.68	148.5	240.4	56.67
15	80.0	170.0	−195.3	75.8	169.9	−197.4
16	80.0	90.0	−174.6	80.5	89.1	−174.7
17	50.0	220.0	−190.8	52	219.3	−190.9
5	320.0	250.0	−173.12	324.6	268.6	−173.75

simulations concurred. Structures containing the dihalo-triazinyl functionality were found to have a much deeper potential energy well, i.e. much lower energies than are found for the previous series. The phenyl-3-azonaphthalene-8-aminodichlorotriazine **15** folds in such a manner that it appears to be effectively self-encapsulate, with torsion values from the GRID-scan searches of 80 and 90° for Φ_1 and Φ_2, respectively. The addition of a hydroxyl group adjacent to the azo-linkage in **15**, to give phenyl-3-azonaphtha-1-ol-8-aminodichlorotriazine **16**

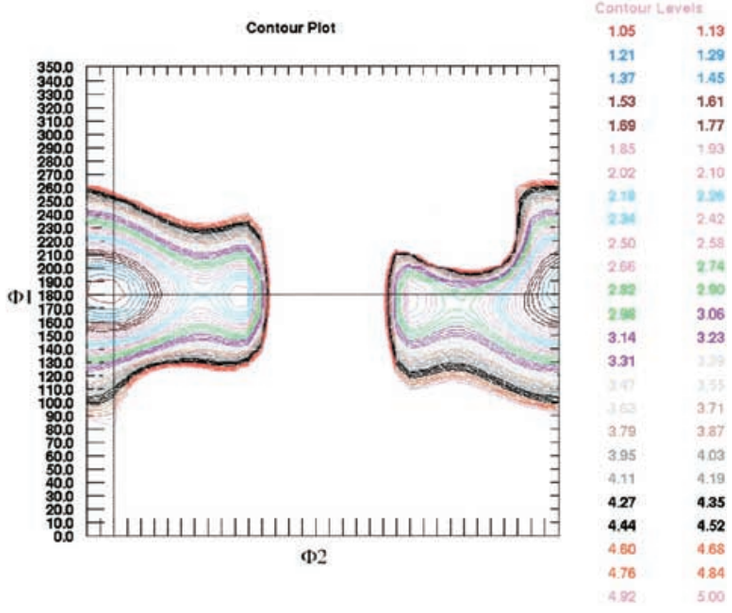

FIGURE 5 GRID-scan plot for phenylazonaphth-1-ol **12**.

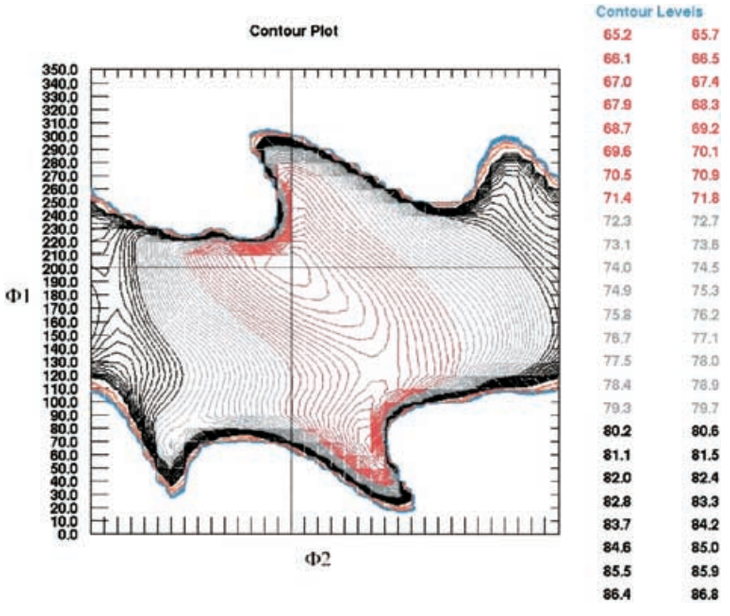

FIGURE 6 GRID-scan plot for phenylazonaphthalene-3,6-disulphonate **13**.

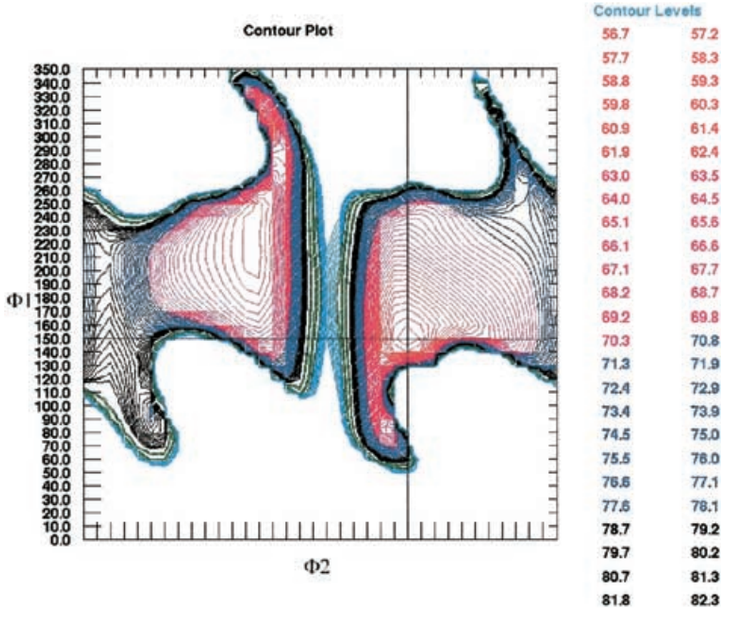

FIGURE 7 GRID-scan plot for phenylazonapth-1-ol-3,6-disulphonate **14**.

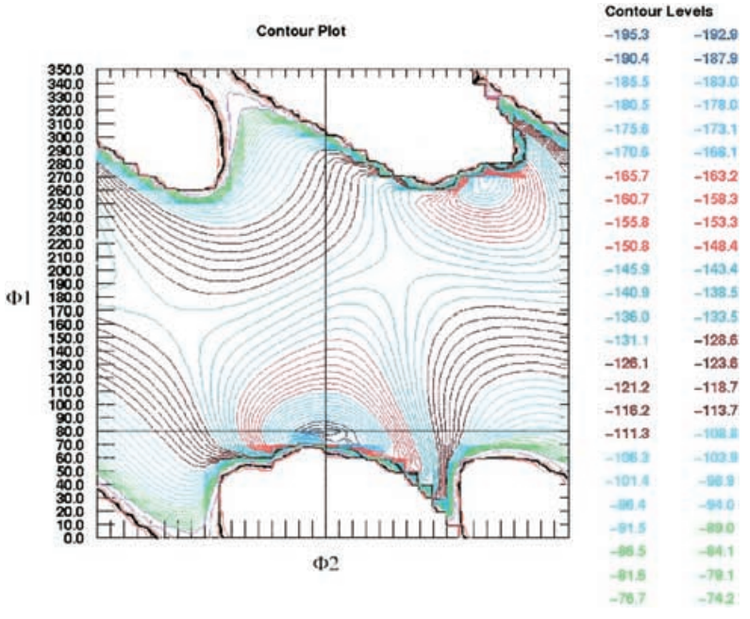

FIGURE 8 GRID-scan plot for phenyl-3-azonaphthalene-8-aminodichlorotriazine **15**.

(Fig. 9), had a similar effect upon Φ_2 to that observed with phenylazonaphth-1-ol **12**, although not as substantial. Following the pattern established with structures **11**–**14**, phenyl-3-azonaphthalene-8-aminodichlorotriazine-3,6-disulphonate **17** (Procion Red MX-5B missing the hydroxyl) was subjected to GRID-scan conformational analysis, and the results were not too dissimilar to those for phenyl-3-azonaphthalene-8-aminodichlorotriazine **15** (Fig. 10).

The results for Procion Red MX-5B **5** (Fig. 11), on initial inspection, appear to be drastically different to those already discussed. However, the results are essentially the same as for the other systems containing the dichlorotriazinyl functionality within the confines of the torsional angle window for Φ_1 having a value of 320°, which is effectively equivalent to −40°. Additionally Φ_2 is 250°, which is comparable to that observed for the same torsion in phenylazonaphth-1-ol-3,6-disulphonate **13**. This indicates that the major effects upon Φ_1 arise from the dichlorotriazinyl ring, whereas the factors affecting Φ_2 derive mainly from the effects of the hydroxyl group.

The result of the GRID-scan searches and molecular dynamics studies can be readily compared with each other, as shown in Table III. From these results, it can be seen that the GRID-scan results are in agreement with those obtained for the molecular dynamics analyses of same structures **11**–**17**. These concurring results

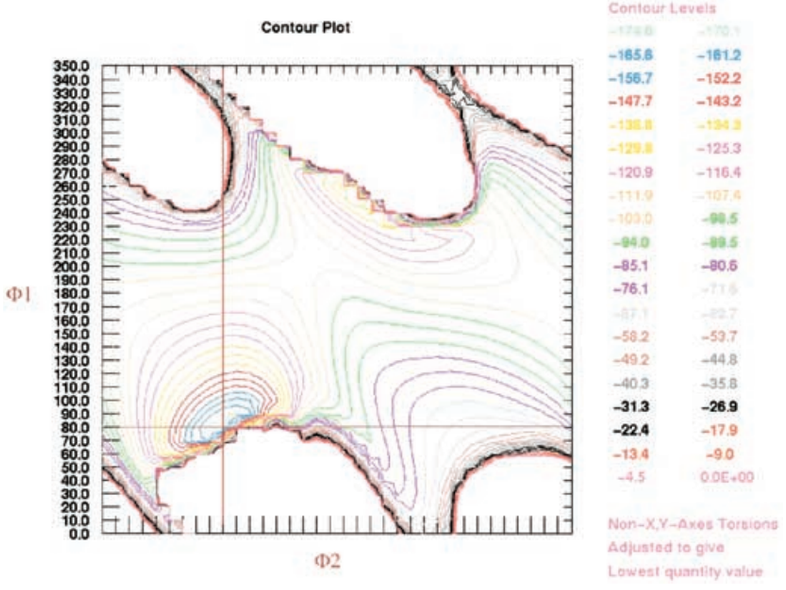

FIGURE 9 GRID-scan plot for phenyl-3-azonaphthalene-8-aminodichlorotriazine **16**.

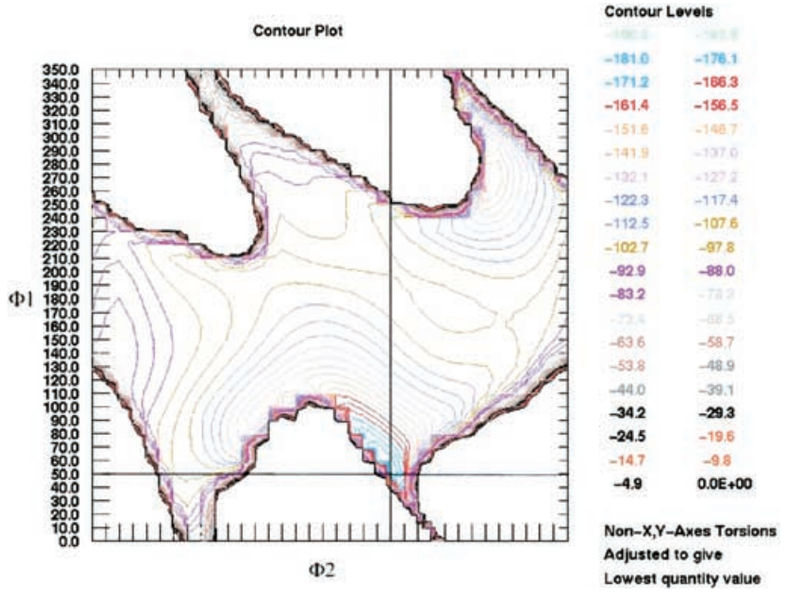

FIGURE 10 GRID-scan plot for phenyl-3-azonaphthalene-8-aminodichlorotriazine-3,6-disulphonate **16**.

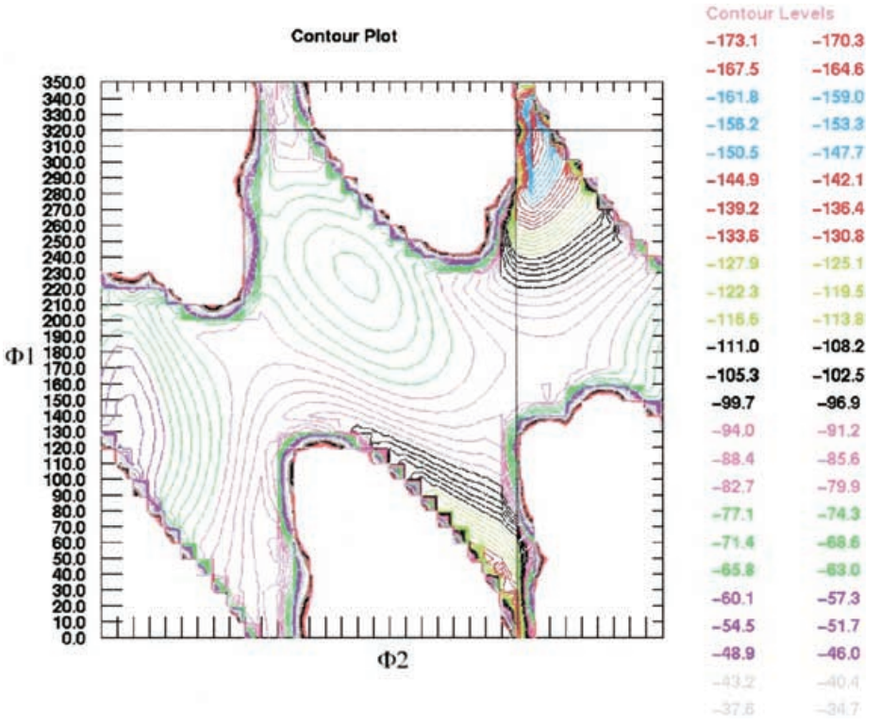

FIGURE 11 GRID-scan plot for Procion Red MX-5B **5**.

provide a good indication of the validity of the modelling studies using molecular dynamic methods and the CHARMm force field on such complex azo dye-related systems.

CONCLUSION

From the results presented herein it is possible to conclude that the azo-linkage is not as rigid as conventional wisdom perhaps indicates. There is considerable freedom of movement around the C–N=N–C dihedral and the favoured arrangement is heavily dependent upon other substituents and hence repulsive interaction within the molecule. The ease of torsional variation around the azo-linkage implies that orbital overlap in the formerly sp^2-hybridised system is relatively weak. This deformation from ideality (i.e. 0 and 180° for a *cisoid*- versus *transoid*-conformation, respectively) can be brought about by a number of factors, such as intramolecular steric repulsions and keto–enol tautomerism (in the case of *ortho*-hydroxy azo-compounds). Despite the flexibility of azo-linked aromatic systems, CHARMm readily reproduces solid-state structures within 5% error and can be expected to be a reliable modelling tool for predicting the geometric preferences for new structures. Subsequent studies will be reported where CHARMm is used to model dye-aggregation and recognition phenomena in due course; such studies are key to a fundamental understanding of the mechanism of dyeing processes.

EXPERIMENTAL

General Computational Procedures

All molecular modelling work was undertaken on a Silicon Graphics O_2 workstation with a 180 MHz CPU, 64 Mb of RAM running IRIX 6.2. QUANTA® was used in the initial stages and was upgraded to QUANTA 97®. Hardcopies of structures were prepared using Snapshot for screen capture and XV for RGB to JPEG conversion.

Comparison of Free and Locked Keto–enol Tautomers of 1-phenyl Azo-napthalene Derivatives

Two-dimensional structures of 1-(4-methylphenylazo)napthalene-2-acetate **9** and 1-(4′-*N*,*N*-dimethylaminophenylazo)-2-napthol **10** were constructed using the 2D

interface within QUANTA 97® these structures were then transferred to the three-dimensional interface before gas phase minimisation over 4000 iterations using the SD algorithm to remove high energy interactions, then the minimisation was repeated using the CG algorithm again until the structure reached its minimum energy according to the CHARMm force field. Molecular dynamics simulations were then performed over a 4 ps time scale, for each of the stages, heating to 300 K, equilibration and simulation at 300 K. Simulated annealing was undertaken upon completion of the dynamics simulations, by repeat minimisation of the dynamics output using the CG algorithm until the structure would minimise no further and the results for the two structures compared.

Gas Phase Minimisation Studies of Procion Red MX-5B (azo-phenol Form)

A Procion Red MX-5B **5** molecule was constructed using the two-dimensional molecular editor interface within QUANTA 97®. This was then subjected to gas phase minimisation over 4000 iterations using the SD algorithm to remove high energy interactions, then the minimisation was repeated using the CG algorithm again until the structure reached its minimum energy according to the CHARMm force field.

Gas Phase Molecular Dynamics Studies of Procion Red MX-5B (azo-phenol Form)

Using the CG minimisation output from procedure of "Gas phase minimisation studies of Procion Red MX-5B (azo-phenol form)" section molecular dynamics simulations were performed. The dynamics simulations were run over a 4 ps time scale, for each of the stages, heating to 300 K, equilibration and simulation at 300 K. Simulated annealing was undertaken upon completion of the dynamics simulations, by repeat minimisation of the dynamics output using the CG algorithm until the structure would minimise no further.

Conformational Analysis of Procion Red MX-5B and Its Substructures by GRID-scan Searching

Conformation analysis was performed using structures that had been created using the molecular editor and subjected to minimisation, dynamics and annealing. These structures were then subjected to conformational analysis by periodic rotation about one torsion Φ_1 in 10° increments through a full 360° and sequential rotation of a second torsion Φ_2 also by 10° until 360° rotation had been

completed. The energy of each of the conformations was recorded and plotted as a two-dimensional contour map for each structure.

Conformational Analysis of Procion Red MX-5B and Its Substructures by Minimisation-dynamics-minimisation Methods

Structures **5** and **11**–**17** were constructed within the two-dimensional molecular editor interface within QUANTA 97® and subjected to minimisation, these structures were then subjected to molecular dynamics simulations as described above and then re-minimised using the minimisation method in "Gas phase minimisation studies of Procion Red MX-5B (azo-phenol form)" section and the results recorded.

References

[1] Hartlet, G.S. (1937) "The *cis* form of azobenzene", *Nature* **140**, 281.
[2] Hartley, G.S. (1938) "The *cis* form of azobenzene and the velocity of the thermal *cis*–*trans* conversion of azobenzene and some derivatives", *J. Chem. Soc.*, 633.
[3] Zimmerman, G., Chow, L.Y. and Paik, U.J. (1958) "The photochemical isomerisation of azobenzene", *J. Am. Chem. Soc.* **80**, 3528.
[4] Schulte-Frohlinde, D. (1957) "Mechanism of the catalytic *cis*–*trans* rearrangement of azobenzene", *L. Ann. Chem.* **612**, 131.
[5] Jaffé, H.H. (1966) "The electronic structure and spectra of *cis* and *trans* azobenzene", *J. Am. Chem. Soc.* **88**, 1948.
[6] Hamlin, J.D., Phillips, D.A.S. and Whiting, A. (1999) "UV/Visible spectroscopic studies of the effects of common salt and urea upon reactive dye solutions", *Dyes Pigm.* **41**, 137.
[7] Cambridge Crystallographic Database, accessed via "QUEST" stored at the Daresbury Laboratory.
[8] Mostad, A. and Romming, C. (1971) "On the structure of L-dopa [2*S*-3(3,4 dihydroxyphenyl)alanine]", *Acta Chem. Scand.* **25**, 3561.
[9] Kobelt, D., Paulus, E.F. and Kunstmann, W. (1972) "X-ray single crystal structure analysis of 1-(2,5 dichlorophenylazo)-2-hydroxy-3-napthoic acid and 4-chloro-2,5-dimethoxyanilide chlorine derivatives of permanent brown FG", *Acta Crystallogr., Sect. B* **28**, 1319.
[10] Zenki, M., Shibahara, T., Yamasaki, M. and Kushi, Y. (1990) "X-ray analysis, crystal structure of arsenazo-I", *Anal. Sci.* **6**, 153.
[11] Flower, K.R., Cross, W.I. and Pritchard, R.G. (1999) "Tautomerisation in 1-(4-methylphenylazo)napthalen-2-ol & 2-(4-methylphenylazo)4-methylphenol: a crystallographic and C13 {H-1} NMR study", *J. Chem. Res.* **5**, 178.
[12] Olivieri, A.C., Wilson, R.B., Paul, I.C. and Curtin, D.Y. (1989) "C13 NMR and X-ray structure determination of 1-(arylazo)-2-napthols intramolecular proton transfer between nitrogen and oxygen atoms in the solid state", *J. Am. Chem. Soc.* **111**, 5525.
[13] Quanta forcefield engines—CHARMm principles, Molecular Simulations Inc., San Diego, 1997.
[14] Hoover, W.H. (1985) "Canonical dynamics: equilibration phase-space distributions", *Phys. Rev.* **A31**, 1695.
[15] Fletcher, R. and Reeves, C.M. (1964) "Function minimisation by conjugate gradient", *Comput. J.* **7**, 149.
[16] Hooft, R.W.W., Van Eijck, P. and Kroon, J. (1992) "Use of molecular dynamics methods in conformational analysis: glycol a model study", *J. Chem. Phys.* **97**, 3639.